ISSN: (Print) (Online) Journal homepage: <https://www.tandfonline.com/loi/tbsd20>

# Anti-quorum sensing activity in *Pseudomonas aeruginosa* PA01 of benzimidazolium salts: electronic, spectral and structural investigations as theoretical approach

Ebru Önem, Burak Tüzün & Senem Akkoç

To cite this article: Ebru Önem, Burak Tüzün & Senem Akkoç (2022) Anti-quorum sensing activity in *Pseudomonas aeruginosa* PA01 of benzimidazolium salts: electronic, spectral and structural investigations as theoretical approach, Journal of Biomolecular Structure and Dynamics, 40:15, 6845-6856, DOI: [10.1080/07391102.2021.1890222](https://doi.org/10.1080/07391102.2021.1890222)

To link to this article: <https://doi.org/10.1080/07391102.2021.1890222>



View supplementary material [↗](#)



Published online: 01 Mar 2021.



Submit your article to this journal [↗](#)



Article views: 337



View related articles [↗](#)



View Crossmark data [↗](#)



Citing articles: 5 View citing articles [↗](#)



# Anti-quorum sensing activity in *Pseudomonas aeruginosa* PA01 of benzimidazolium salts: electronic, spectral and structural investigations as theoretical approach

Ebru Önem<sup>a</sup>, Burak Tüzün<sup>b</sup> and Senem Akkoç<sup>c</sup> 

<sup>a</sup>Faculty of Pharmacy, Department of Pharmaceutical Microbiology, Suleyman Demirel University, Isparta, Turkey; <sup>b</sup>Faculty of Sciences, Department of Chemistry, Cumhuriyet University, Sivas, Turkey; <sup>c</sup>Faculty of Pharmacy, Department of Basic Pharmaceutical Sciences, Suleyman Demirel University, Isparta, Turkey

Communicated by Ramaswamy H. Sarma

## ABSTRACT

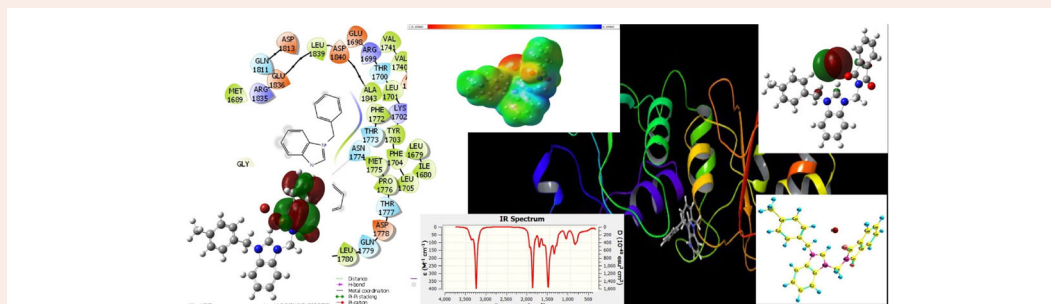
Quorum sensing (QS) is a system used in the expression of virulence factors by many pathogenic bacteria, and blockage of the system is seen as a new and effective strategy in combating with resistant bacteria. The inhibition effects of two benzimidazolium salts, namely 1-(2-methylbenzonitrile)-3-benzylbenzimidazolium bromide (**2**) and 1-(*N*-methylphthalimide)-3-(4-methylbenzyl)benzimidazolium bromide (**3**), on quorum sensing-related virulence factors such as pyocyanin, elastase, biofilm formation and swarming motility, which is an opportunistic pathogen *Pseudomonas aeruginosa* PA01, were investigated in this study. The results show that the compound **3** has a significant inhibition on biofilm formation with 94%. Furthermore, the compounds **2** and **3** reduced swarming motility by 64–69% as well as pyocyanin production by 49–64% in *P. aeruginosa* PA01 without preventing bacterial growth in the tested concentrations. HF, B3LYP and M06–2X methods were used with 3–21 g, 6–31 g, sdd basis sets to compare the chemical activity of the compounds. Theoretically, <sup>1</sup>H NMR, <sup>13</sup>C NMR and Infrared spectra of the compounds were calculated in the HF/6-31++g basis set. The biological activities of the relative compounds were theoretically studied against cancer proteins. Crystal structure of the BRCT repeat region from the breast cancer associated protein, ID: 1JNX, crystal structure of liver cancer protein, ID: 3WZE and crystal structure of lung cancer protein, ID: 5ZMA, were compared. In the docking studies, the best result was obtained with compound **2** against the lung cancer cell with a docking score parameter of –5.85.

## ARTICLE HISTORY

Received 9 September 2020  
Accepted 9 February 2021

## KEYWORDS

Cancer protein; DFT; molecular docking; LasR protein; quorum sensing inhibitors




## 1. Introduction

The benzimidazole derivatives have been used in various biological activity applications such as anticancer (Akkoç, 2019a, 2019b, 2021), pancreatic lipase inhibitor agents (Menteşe et al., 2018), in the treatment of Alzheimer's disease (Fang et al., 2019), antitubercular (Desai et al., 2014) and antibacterial agents (Gök et al., 2019).

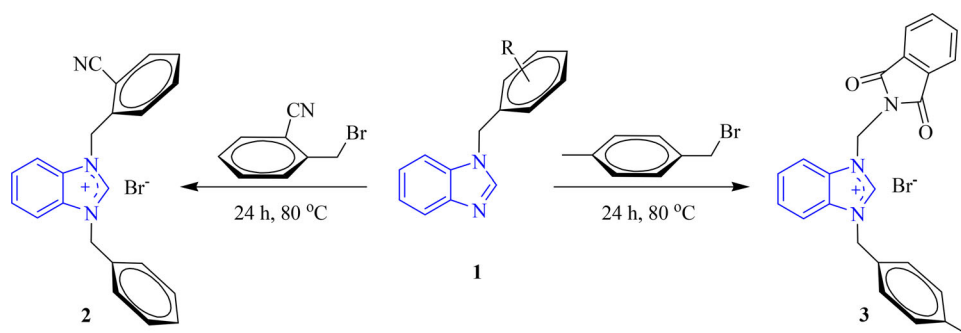
Antibiotics, which have been used to fight with bacterial infections for many years, have lost their effectiveness as a

result of misuse. Many new strategies have been tried against bacteria to date, and one of the most effective is thought to be the inhibition of bacterial communication (Jiang et al., 2019). *P. aeruginosa* creates an effective infection process by synthesizing many virulence factors through bacterial communication known as QS network (Kostylev et al., 2019). In this network, signaling molecules, also known as auto-inducers, are synthesized by bacteria and released out of the cell to be sensed by a bacteria's own receptors and the other bacteria (Hentzer & Givskov, 2003). There are

**CONTACT** Senem Akkoç  [senemakkoc@sdu.edu.tr](mailto:senemakkoc@sdu.edu.tr); [senemakkoc44@gmail.com](mailto:senemakkoc44@gmail.com)  Faculty of Pharmacy, Department of Basic Pharmaceutical Sciences, Suleyman Demirel University, Isparta 32260, Turkey

 Supplemental data for this article can be accessed online at <https://doi.org/10.1080/07391102.2021.1890222>

© 2021 Informa UK Limited, trading as Taylor & Francis Group



**Scheme 1.** Synthesis of compounds **2** and **3**.

two main systems in *P. aeruginosa*, *las* and *rhl*, which are hierarchically related to each other (Bratu et al., 2006). In the *las* system, the transcriptional regulatory protein is LasR and the auto-inducing molecule N-(3-oxododecanoyl)-L-homoserine lactone (3-oxo-C<sub>12</sub>-HSL), while the *rhl* system contains RhIR and RhII as activator proteins and is responsible for the synthesis of N-butanoyl-L-homoserine lactone (C<sub>4</sub>-HSL) (Ahmed et al., 2019). Both systems are closely linked to each other and are known to regulate the production of some virulence factors, such as swarming motility, biofilm formation, elastase, alkaline protease, exotoxin A, rhamnolipids, pyocyanin (Smith et al., 2002; Venturi, 2006).

Over the last years, the difficulty of controlling infectious diseases due to their resistance to antibiotics has made it necessary to produce of novel strategies and QS inhibition has emerged as an effective option. Unlike conventional antibiotics, QS inhibitors (QSIs) do not inhibit bacterial growth and fight bacteria by blocking communication between bacteria. For this purpose, many synthetic materials were tested as QSIs, and strong inhibition effect was observed in studies with AHL analogs (Hentzer & Givskov, 2003; Morohoshi et al., 2007; Seyhan et al., 2017; Wang et al., 2008).

Nowadays, the most common method of comparing the chemical and biological activities of molecules is theoretical calculations as it is both faster and cheaper. Therefore, theoretical studies are a good guide to experimental studies. Numerical values of many theoretical parameters containing a lot of information about the molecule were obtained with these theoretical calculations (Günsel et al., 2020).

In the present study, the inhibitory effect of benzimidazole-derivatives on the production of elastase and pyocyanin (QS-regulated virulence factors), the formation of biofilm and swarming motility in *P. aeruginosa* PA01 were investigated. It attempted to account for their potential interactions with the *LasR* protein by molecular modeling. Furthermore, the optimized structures of the compounds (**2**, **3**) were obtained by using the Gaussian package program. Quantum chemical parameters of the compounds were calculated by optimized structures. The biological activities of the compounds **2**, **3** against proteins were compared. These proteins are crystal structure of the BRCT repeat region from the breast cancer associated protein, ID: 1JNX (Williams et al., 2001), crystal structure of VEGFR kinase (liver cancer) protein, ID: 3WZE (Okamoto et al., 2015) and crystal structure of an allosteric Eya2 phosphatase inhibitor (lung cancer) protein, ID: 5ZMA (Anantharajan et al., 2019).

## 2. Materials and methods

### 2.1. Synthesis of benzimidazolium salts

The synthesis of these two known compounds was conducted according to the literature protocols (Akkoç, Gök, et al., 2016; Akkoç, Özer İlhan, et al., 2016). Potassium hydroxide (1.5 mmol) was added to the solution of benzimidazole in ethyl alcohol. Following this, aryl/alkyl halide (1 mmol) was added to over this reaction mixture. The N-alkylbenzimidazole was purified via crystallization in ethyl alcohol. Benzimidazolium salts were synthesized from N-alkylbenzimidazole (1 mmol) and aryl halides in DMF. The products were purified by crystallization in a mixture of ethyl alcohol-diethyl ether. The open structure of compounds **2**, **3** is given in Scheme 1.

#### 2.1.1. 1-(2-Methylbenzonitrile)-3-benzylbenzimidazolium bromide, **2**

Colourless compound **2** (404.3 g/mol) was prepared from 1-benzylbenzimidazole (1.15 g, 1 mmol) and 2-(bromomethyl)benzonitrile (1.08 g, 1 mmol) in DMF (Akkoç, Özer İlhan, et al., 2016). The melting point of the relative compound is 235–236 °C.

#### 2.1.2. 1-(N-Methylphthalimide)-3-(4-methylbenzyl)benzimidazolium bromide, **3**

Colourless compound **3** (462.34 g/mol) was synthesized from 2-((1H-benzo[d]imidazol-1-yl)methyl)isoindoline-1,3-dione (1 g, 1 mmol) and 4-methylbenzyl bromide (0.558 g, 1 mmol) in DMF (Akkoç, Gök, et al., 2016). The melting point of the relative compound is 244–245 °C.

## 2.2. QS-related virulence factor assay

### 2.2.1. Elastase assay

Elastase inhibition activity was performed according to Elastin Congo Red (ECR, Sigma) assay protocol (Ohman et al., 1980). *P. aeruginosa* PA01 was grown in Luria Bertani (LB) broth with compounds (2.3–1.5 mM) at 37 °C for 16 h. Centrifugation was done in 15,000 rpm at 4 °C for 10 min. Hundred microliter of supernatant was added to 900 µL of buffer (100 mM Tris, 1 mM CaCl<sub>2</sub>, pH: 7.5, containing 10 mg of ECR). The mixture was incubated at 37 °C for 3 h by shaking

at 200 rpm. Supernatant without indissoluble ECR was measured at 495 nm.

### 2.2.2. Pyocyanin assay

The tested PA01 strain was produced in LBB medium at 37 °C for 16–18 h. The compounds (**2**, **3**) to be tested were added to bottles with 10 mL of LBB medium in a final concentration of 1.5 mM, together with the PA01 culture set at 0.05 OD at 600 nm. It was incubated by shaking at 37 °C for 16–18 h. After incubation, 5 mL of *P. aeruginosa* culture was extracted from 3 mL of chloroform and 2 mL of organic phase was separated into a clean tube (Essar et al., 1990). A new pyocyanin-rich phase was obtained by adding 1 mL of 0.2 M HCl to the separated phase. Optical density results at 520 nm were recorded by reading the amount of pyocyanin in the extract. The results were evaluated by comparison with the PA01 strain. The pyocyanin test was repeated three times for each samples and the average of the obtained results was taken.

### 2.2.3. Swarming motility assay

According to swarming motility assay (Rashid & Kornberg, 2000), 100 µL of compounds (1.5 mM final concentration) was added to 20 mL of swarming medium (consisted of 8 g/L nutrient broth, 5 g/L bacto agar and 0.5% (w/v) glucose). Five microliter of the supernatant of bacterial culture, which was held overnight, was dropped into the middle of the swarm medium. Then, the plates were incubated for an overnight at 37 °C. The inhibition effect of compounds was evaluated by measuring the diameter of the swarming from the inoculation site.

### 2.2.4. Biofilm test

The microplate spectrophotometry was used for the biofilm test (O'Toole, 2011). The compounds (**2**, **3**) together with 5 µL of the *P. aeruginosa* PA01 culture were added to wells containing LB broth at a final concentration of 1.5 mM. It was incubated at 37 °C for 48 h. After incubation, the microplates were flipped over to discharge the contents of the wells. The emptied wells were rinsed three times with distilled water and then the plate was dried. The biofilm-associated cell residues were stained with 0.1% crystal violet. The wells were emptied again and rinsed three times with pure water. To quantitatively determine the biofilm formation, 95% ethyl alcohol was added to microplates. To find the optical density value of each well, the readings were conducted at 570 nm after 15 min.

## 2.3. Theoretical method

### 2.3.1. Gaussian study

The theoretical methods give many information about molecules. The programs GaussView 5.0.8, ChemDraw Professional 15.1, Gaussian09 AS64L-G09RevD.01 and Chemcraft V1.8 package were used in this study (Chemissan Version 4.43 package, Dennington et al., 2016; Frisch et al., 2009;

PerkinElmer, 2012; Leonid, 2017). The compounds (**2**, **3**) were calculated using the Hartree–Fock (HF) (Vautherin & Brink, 1972), Becke, 3-parameter, Lee–Yang–Parr (B3LYP) (Becke, 1993; Stephens et al., 1994; Wiberg, 2004), M06–2X (Hohenstein et al., 2008) methods with 3–21 g, 6–31 g and added to basis set. With the calculations of compounds using the Gaussian software program, many parameters were obtained. Highest Occupied Molecular Orbital (HOMO) and Lowest Unoccupied Molecular Orbital (LUMO) values are the most significant among the parameters. Because, information about the chemical activities of compounds can be calculated using HOMO and LUMO parameters. Quantum chemical parameters such as  $E_{\text{HOMO}}$ ,  $E_{\text{LUMO}}$ ,  $\Delta E$  (HOMO-LUMO energy gap), chemical hardness ( $\eta$ ), chemical potential ( $\mu$ ), nucleophilicity ( $\epsilon$ ), electronegativity ( $\chi$ ), electrophilicity ( $\omega$ ), global softness ( $\sigma$ ) and proton affinity (PA) are obtained from the quantum chemical calculations.

### 2.3.2. DFT method

The DFT method is a different method from the *ab initio* method in theoretical calculations. Because, the DFT method resolves both the energy of a molecule for its electron density and describes it without evaluating it from the total wave function.

### 2.3.3. Docking study

One of the most common and quality methods used to evaluate the biological activities of compounds is molecular docking. The biological activities of compounds **2** and **3** against the proteins of cancer cells were compared using molecular docking calculation method. As a result of these calculations, many parameters about the biological activities of compounds were obtained, which were derived from the interaction of molecules and proteins.

The molecules need to be prepared for the docking calculations. It was calculated using the Gaussian software program (Frisch et al., 2009) to find the optimized structures of molecules. Then, files with the \*.sdf extension were created using these optimized structures. Using these files, calculations were done with Maestro Molecular modeling platform (version 12.2) (Schrodinger, 2019). This platform has come together with many modules. In the first module, the proteins to be examined must be prepared for calculations. The protein preparation module (Friesner et al., 2006; Schrödinger, LLC, 2019; Schrödinger Release 2019-4, 2016) is used for this calculation. The proteins of the cancer cells consist of many proteins. The proteins used in this study were crystal structure of the BRCT repeat region from the breast cancer associated protein, ID: 1JNX, crystal structure of liver cancer protein, ID: 3WZE and crystal structure of lung cancer protein, ID: 5ZMA. The LigPrep module (Sastry et al., 2013; Schrödinger Release 2019-4, 2019) was used to prepare the molecules for molecular docking calculations. The prepared compounds and proteins were docked with each other. The Glide ligand docking module (Du et al., 2020) was used for the docking of compounds and proteins.

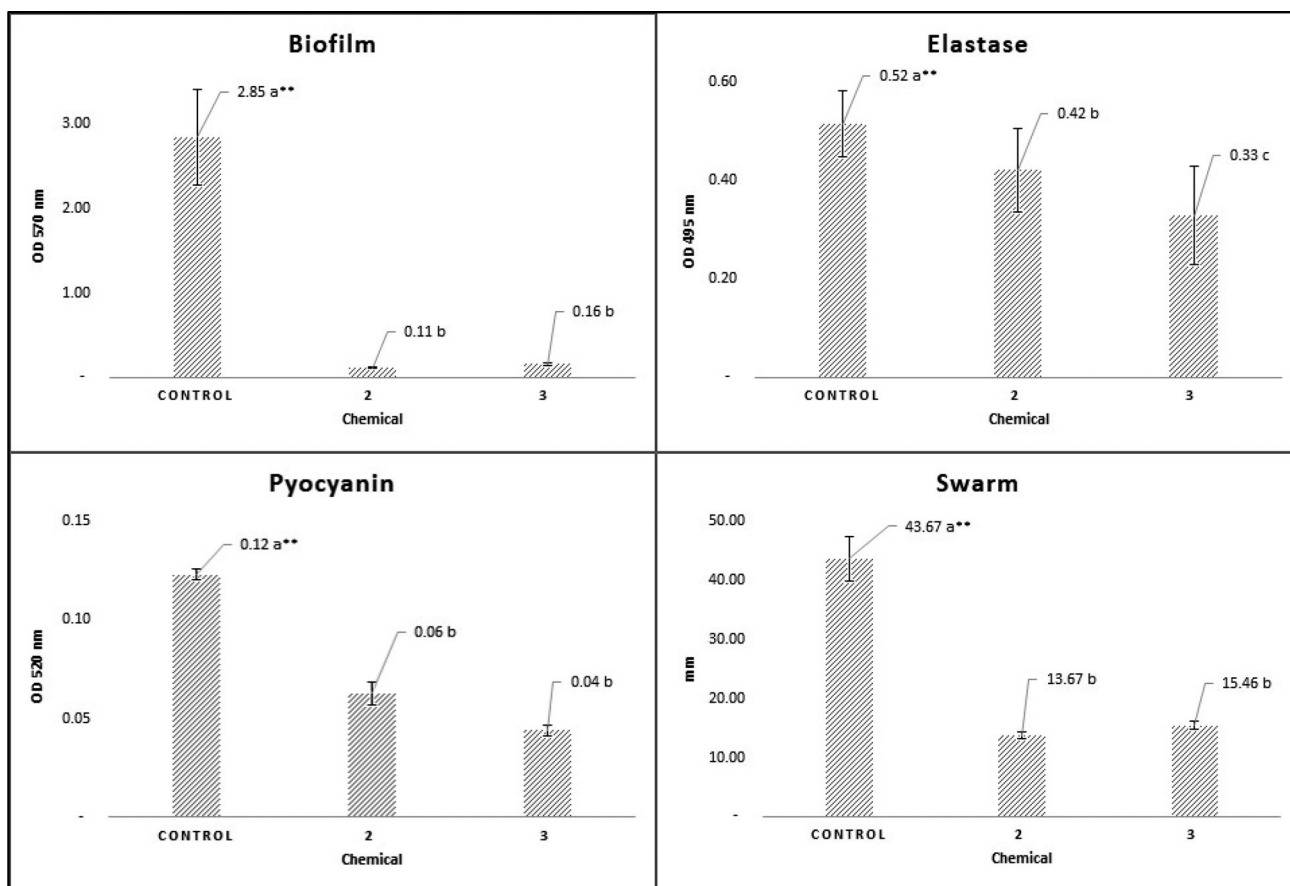


**Figure 1.** Inhibition effect of compounds on elastase, pyocyanin production, biofilm formation and swarming motility. \*\*Differences between mean values followed by different letters of compounds are statistically significant at  $p < .01$ .

### 3. Results and discussion

#### 3.1. Inhibition of virulence factors

Antibiotics are used after the infection develops, and QS inhibitors prevent the formation of virulence by blocking communication between bacteria's. Therefore, doses or molecules that are not effective on bacterial growth are used in conducted studies with compounds used as QS inhibitors. Before starting the inhibition effect of the activity tests of virulence factors, the concentration at which the bacterial growth was not inhibited was determined by the minimum inhibition concentration (MIC) test. Compounds (**2**, **3**) were used at a concentration level of 1.5 mM. The relative compounds investigated as potential QSIs showed different inhibitory effects on all virulence factors (Figure 1).

*Pseudomonas aeruginosa* is an opportunistic pathogen that causes chronic lung diseases. Elastase enzyme gives rise to the spread of infection by causing local tissue damage (Kuang et al., 2011; Nomura et al., 2014). According to the elastase test results, it was observed that the production of elastase in the samples with compounds (**2**, **3**) reduced elastase activity to 18% and 36% for **2** and **3**, respectively.

In recent years, there has been a significant increase in the number of studies aimed to prevent the QS system. During this time, the effect of many natural and synthetic molecules has been investigated. Pyocyanin produced by the QS system is a phenazine-derived pigment that plays a role

in the pathogenesis of *P. aeruginosa* and is responsible for oxidative and neutrophil-related tissue damage in the lungs. In the results of the pyocyanin tests conducted within the scope of this study, the inhibition effect of **2** on pyocyanin production was obtained as 49% while the inhibition rate of **3** was found to be 64%.

Biofilm protects bacteria against antimicrobial agents and host immune system. It plays an active role in the permanent colonization of bacteria in the host and complicates the host's healing process (Jiang et al., 2019). Studies show that by blocking the communication between bacteria, biofilm formation is prevented and antibiotic resistance is reduced (Hong et al., 2012; Lu et al., 2019). It has been shown that this condition is caused by inhibition of polymer formation, suppression of cell adhesion and attachment, inhibition of the extracellular matrix production (Casilag et al., 2016). Thus, the antibiofilm activities of the compounds were investigated in PA01. In the biofilm test results conducted at 1.5 mM concentration, it was found that samples including compound **3** had a 94% significant inhibition effect on biofilm formation. Inhibition of QS systems generally occurs by three different mechanisms, namely, prevention of AHL production, inactivation of signal molecules and inhibition of AHL signal reception (Rasmussen & Givskov, 2006). Inhibition of receiving the AHL signal molecule can be achieved by natural AHL signaling molecules with the receptor antagonist molecule having the ability to compete for binding to protein. Molecules that compete with AHL are structurally similar



to AHL and act like the AHL binding site, preventing the receptor from being activated. For this purpose, many different molecules have been synthesized and also many existing molecules have been screened with chemo informatics (Blöcher et al., 2018; Nain et al., 2020; Önem et al., 2018). The main ring of the compounds **2** and **3**, of which inhibitory effects were investigated in this study, is similar to the structure of AHL. Therefore, it is thought that possible inhibition will occur in this way. Swarming motility is one of the virulence that plays an important role in the pathogenesis of *Pseudomonas*. According to the swarming motility results, both compounds showed a high rate of inhibition effect (64%, 69%), and all results were found statistically significant (Figure 2).

### 3.2. Gaussian calculation

Theoretical calculations guide many experimental studies at the present time. It is seen that the results obtained from experimental studies are in great harmony with the results obtained from theoretical calculations (Tüzün, 2019). As a result of theoretical calculations, many parameters are obtained. Comparison of the chemical activities of molecules is made with the numerical values obtained as a result of theoretical calculations. These parameters give a lot of information about the chemical activities of molecules. Among these parameters, the most known and used ones are HOMO

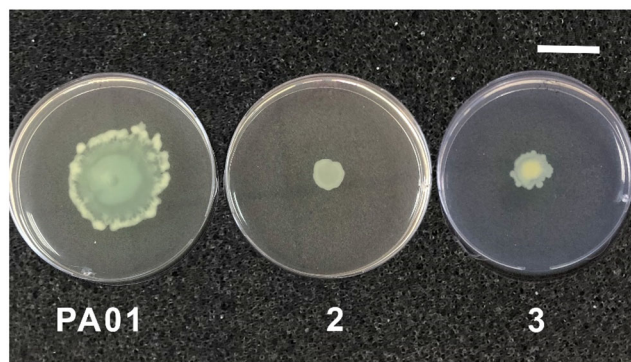


Figure 2. Inhibition effect of compounds on swarming motility in PA01 (Scale bar = 30 mm).

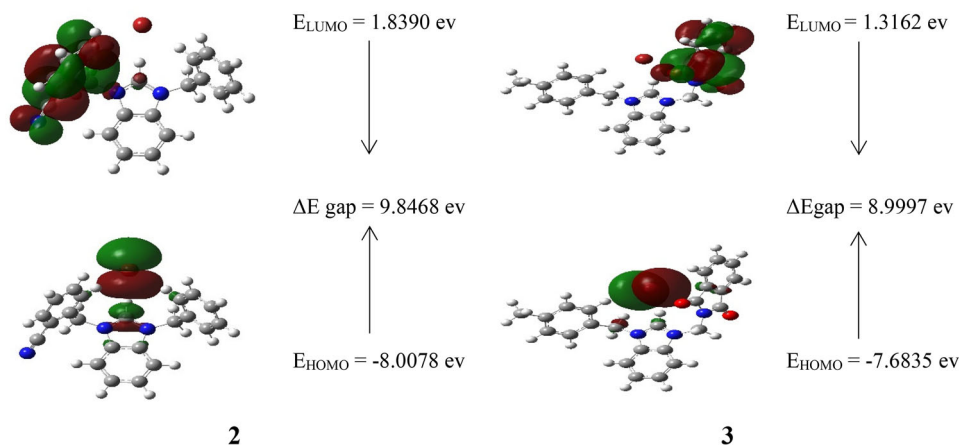


Figure 3. HOMO, LUMO orbitals and their energy gap ( $\Delta E_{gap}$ ) for compounds 2 and 3.

and LUMO. The chemical activity of the molecule with the most positive numerical value of the HOMO parameter is the highest. Because, it will be easier to give electrons in high energy filled molecular orbitals than others. In this way, these molecules will interact more easily and increase their chemical activity (Günsel et al., 2020). The energy gap ( $\Delta E_{gap}$ ) between LUMO and HOMO for compounds 2 and 3 are given in Figure 3.

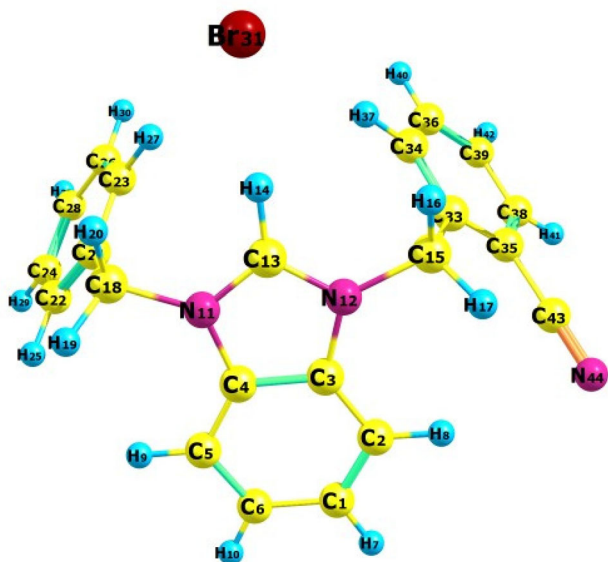
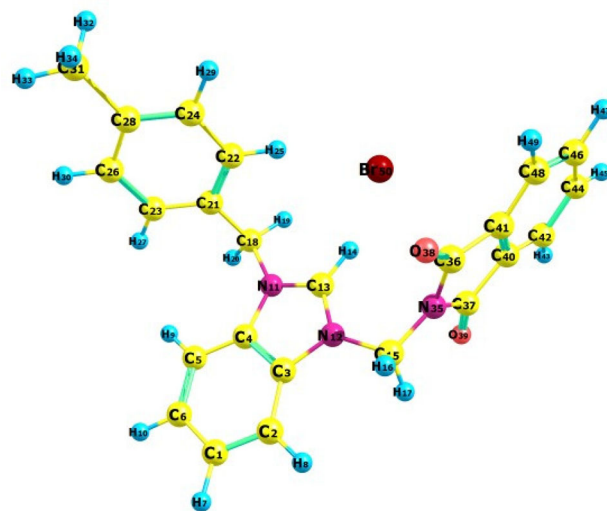
Conversely, the chemical activity of the molecule with the numerical value of the LUMO parameter is the most negative. Because, it will be easier to take electrons in low energy filled molecular orbitals than others. Apart from these parameters, another important parameter is electronegativity, which indicates the power of the molecule to attract bond electrons. If a molecule has a high electronegativity value, the molecule attracts more bond electrons. Many such parameters are obtained from the Gaussian software program. Each of these parameters is used to explain the different properties of the molecule. These parameters and their numerical values are given in Table 1.

### 3.3. NMR spectrum

Nuclear magnetic resonance (NMR) spectroscopy is one of the common methods used to estimate the structure of molecules. In this method, the atoms in the molecule cause vibration according to the atoms around them (Günsel et al., 2019). The structure can be determined from the numerical values formed according to these vibrations. NMR spectroscopy is the numerical value of these vibrations. The studied compounds were calculated using the HF/6-31++g basis set. In these calculations, Gaussian package program was made with the gauge-independent atomic orbital (GIAO) method. With this calculation method, the carbon and hydrogen atoms in the compound have chemical shift values. Calculations were done using gas, methanol ( $\text{CH}_3\text{OH}$ ) and dimethyl sulfoxide (DMSO) solvents in this study. Chemical shift values obtained as a result of the calculations and experimental processes are given in Supporting Information file (Tables S1 and S2). In the experimental processes, NMR spectra were taken at 298 K in 400.13 MHz and 100.13 MHz for  $^1\text{H}$  and  $^{13}\text{C}$  NMR, respectively. Atoms are labeled in

**Table 1.** The calculated quantum chemical parameters of compounds.

	$E_{\text{HOMO}}$	$E_{\text{LUMO}}$	$I$	$A$	$\Delta E$	$\eta$	$\sigma$	$\chi$	$\Pi$	$\omega$	$\varepsilon$	dipol	Energy
<b>B3LYP/3-21g LEVEL</b>													
2	-4.7103	-1.7581	4.7103	1.7581	2.9522	1.4761	0.6775	3.2342	-3.2342	3.5432	0.2822	7.8595	-97128.7476
3	-4.3843	-2.1524	4.3843	2.1524	2.2319	1.1159	0.8961	3.2684	-3.2684	4.7862	0.2089	8.2976	-103295.129
<b>B3LYP/6-31g LEVEL</b>													
2	-5.0902	-1.9029	5.0902	1.9029	3.1873	1.5936	0.6275	3.4966	-3.4966	3.8358	0.2607	8.4149	-97539.4410
3	-4.7639	-2.4256	4.7639	2.4256	2.3383	1.1691	0.8553	3.5948	-3.5948	5.5265	0.1809	8.2626	-103738.093
<b>B3LYP/SDD LEVEL</b>													
2	-5.2453	-2.2512	5.2453	2.2512	2.9941	1.4970	0.6680	3.7483	-3.7483	4.6924	0.2131	10.246	-27929.1092
3	-5.1544	-2.5810	5.1544	2.5810	2.5734	1.2867	0.7772	3.8677	-3.8677	5.8130	0.1720	6.0071	-34129.1088
<b>HF/3-21g LEVEL</b>													
2	-7.5512	1.9682	7.5512	-1.968	9.5194	4.7597	0.2101	2.7915	-2.7915	0.8186	1.2216	9.8945	-96902.7636
3	-7.1518	1.5475	7.1518	-1.547	8.6993	4.3496	0.2299	2.8021	-2.8021	0.9026	1.1079	9.5244	-103035.165
<b>HF/6-31g LEVEL</b>													
2	-8.0078	1.8390	8.0078	-1.839	9.8468	4.9234	0.2031	3.0844	-3.0844	0.9662	1.0350	9.8189	-97309.3556
3	-7.6835	1.3162	7.6835	-1.316	8.9997	4.4998	0.2222	3.1836	-3.1836	1.1262	0.8879	9.3722	-103473.317
<b>HF/SDD LEVEL</b>													
2	-7.8710	1.5824	7.8710	-1.582	9.4533	4.7267	0.2116	3.1443	-3.1443	1.0458	0.9562	7.9595	-27741.6134
3	-7.6103	1.1745	7.6103	-1.174	8.7847	4.3924	0.2277	3.2179	-3.2179	1.1787	0.8484	7.5739	-33906.8096
<b>M062X/3-21g LEVEL</b>													
2	-5.7452	-0.7921	5.7452	0.7921	4.9531	2.4765	0.4038	3.2687	-3.2687	2.1571	0.4636	8.7225	-97118.6115
3	-5.5185	-0.8574	5.5185	0.8574	4.6611	2.3305	0.4291	3.1880	-3.1880	2.1804	0.4586	8.7250	-103282.512
<b>M062X/6-31g LEVEL</b>													
2	-6.5681	-0.9715	6.5681	0.9715	5.5966	2.7983	0.3574	3.7698	-3.7698	2.5392	0.3938	8.7181	-97530.6438
3	-6.0861	-1.1674	6.0861	1.1674	4.9188	2.4594	0.4066	3.6268	-3.6268	2.6741	0.3740	9.4426	-103726.750
<b>M062X/SDD LEVEL</b>													
2	-6.6448	-1.0305	6.6448	1.0305	5.6143	2.8071	0.3562	3.8377	-3.8377	2.6232	0.3812	6.0178	-27917.3756
3	-6.1038	-1.5315	6.1038	1.5315	4.5724	2.2862	0.4374	3.8177	-3.8177	3.1875	0.3137	9.5775	-34114.8020

**Figure 4.** Labeled representation of atoms in the compound 2.**Figure 5.** Labeled representation of atoms in the compound 3.

Figures 4 and 5 to compare experimental and theoretical chemical shift values.

The numerical values obtained as a result of the calculations and experimental operations are plotted. These graphics are given in Figures 6 and 7.  $R^2$  was calculated from these graphs. At the end of the calculations and experimental processes,  $R^2$  values were calculated as 0.99 in gas, methanol and DMSO phases for both compounds.

As a result of the calculations and experimental processes, the chemical shift values of hydrogen atoms bound to aliphatic carbon atoms are between 5.22 ppm and 6.56 ppm (Günsel et al., 2020). Conversely, hydrogen atoms bound to aromatic carbon atoms were found to be between 8.04 ppm and 16.68 ppm. Besides, the chemical shift values of aliphatic

carbon atoms were seen between 46.67 ppm and 50.56 ppm. Conversely, aromatic carbon atoms were found to be between 111.36 ppm and 159.10 ppm. In the literature searches, the chemical shift values of the carbon and hydrogen atoms in the compounds are within the normal ranges (Asgarova et al., 2019; Maharramov et al., 2019; Naghiyev et al., 2020; Yadigarov et al., 2009; Yin et al., 2020).

### 3.4. Infrared spectrum

Infrared spectroscopy is a method used to predict the structure of molecules as a result of vibrations made by atoms or atomic groups. In this method, each atom or group of atoms has its own vibration frequency. The structures of molecules

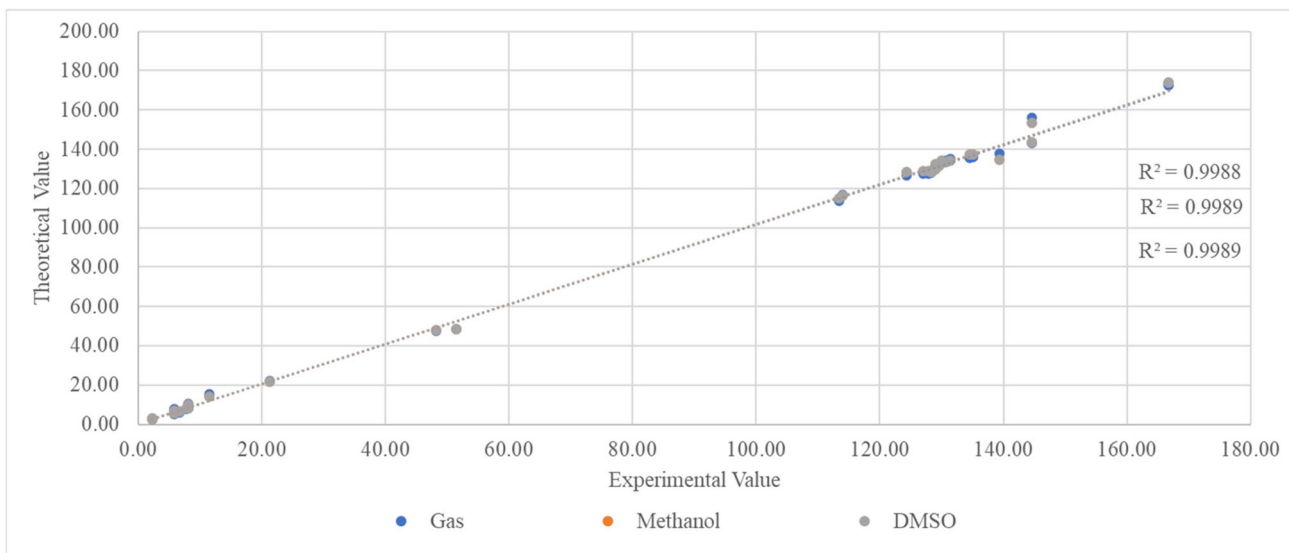


Figure 6. Graphical representation of experimental and theoretical chemical shift values of compound 2.

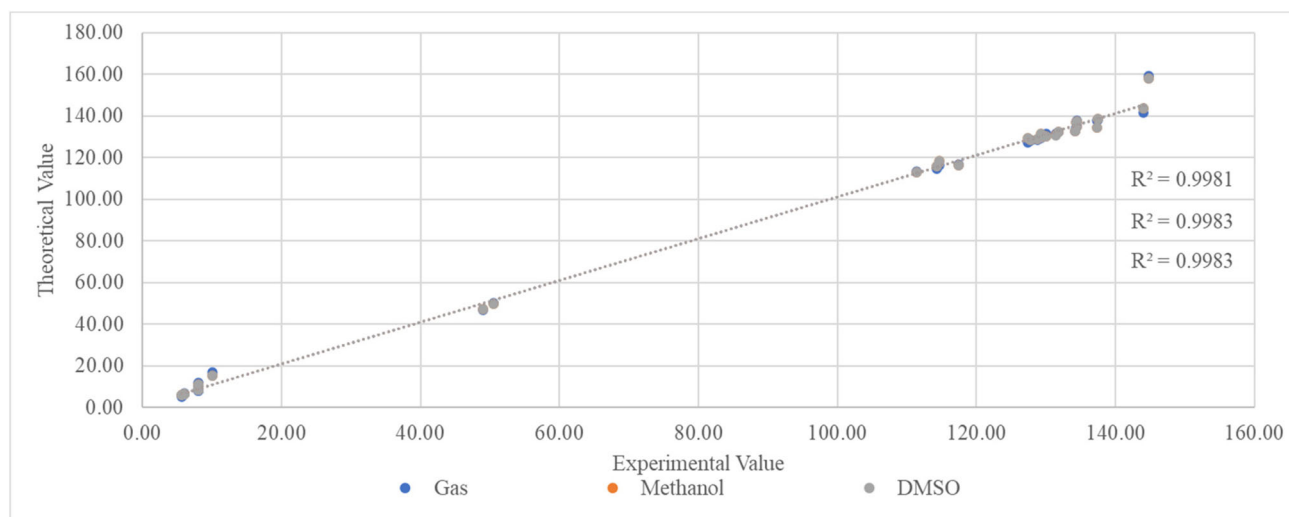


Figure 7. Graphical representation of experimental and theoretical chemical shift values of compound 3.

are determined by the numerical values of these vibrational frequencies. In here, the vibration frequencies of compounds were calculated in gas phase in HF/6-31++g basis set. The spectra obtained as a result of these calculations are given in Supporting Information file with Figures S1 and S2. After the calculations made in the Gaussian software program, the Veda 4XX program (Jamróz, 2004) gives the vibration frequencies of the compounds and vibration modes occur in Table 2.

### 3.5. Molecular docking

Many experimental and theoretical studies are conducted to compare the biological activity of molecules. Among these experimental and theoretical studies, the fastest and the most common is molecular docking (Genc Bilgili et al., 2020). It is possible to compare the biological activities of molecules against proteins with molecular docking calculations. As a result of these calculations, many parameters related to the biological activities of molecules are obtained

Table 2. Selected frequencies of the compounds 2 and 3 at HF/6-31G level.

Compounds	Band	Teo. Freq (cm <sup>-1</sup> )	Vibration modes <sup>a</sup>
2	1	3364	STRE (aromatic CH)
	2	3247	STRE (aliphatic CH)
	3	1899	STRE (O-C)
	4	1739	BEND (H-C-N)
	5	1525	BEND (C-N-C)
	6	1387	STRE (C-C)
	7	1095	STRE (N-C)
	8	879	TORS (H-C-C-C)
	9	632	BEND (C-N-C)
	10	171	STRE (Br-H)
	11	160	BEND (Br-H-C)
3	1	3340	STRE (aromatic CH)
	2	3221	STRE (aliphatic CH)
	3	2532	STRE (N≡C)
	4	1747	BEND (H-C-N)
	5	1604	STRE (N-C)
	6	1544	BEND (H-C-C)
	7	1399	STRE (N-C)
	8	1112	BEND (C-C-C)
	9	845	TORS (H-C-C-C)
	10	638	BEND (N-C-C)
	11	159	BEND (Br-H-C)
	12	126	STRE (Br-H)



(Tüzün, 2020). By comparing the numerical values of these parameters, a lot of information about the molecules is obtained. Among these parameters, the most important ones are docking score and glide emodel parameters. The numerical values of relative parameters give information about biological activity. The molecule with the most negative

numerical value of these parameters has the highest biological activity value (Liu et al., 2020). The high biological activity of compounds demonstrates the highest interaction between proteins and molecule.

The first parameter derived from molecular docking calculations is the docking score, which is used to explain the biological activities of molecules. Other parameters can be listed as follows. Glide Ligand Efficiency is a numerical value of the activity of molecules. Glide Hbond is the numerical value of the number of hydrogen bonds that occur in the interactions of molecules with proteins (Liu et al., 2020). Glide Evdw is the numerical value of van der Waals interactions between molecules and proteins. Glide Emodel is the numerical value of the interaction model between the molecule and proteins. The last parameter obtained from the molecular docking calculations is Glide Einternal, which is the numerical value of the combination of many parameters obtained (Genc Bilgili et al., 2020; Taslimi et al., 2020). All parameters obtained are given in Table 3.

The interactions between compounds and proteins are given in Figures 8–13. There are many different interactions such as hydrogen bonds, polar and hydrophobic interactions,  $\pi$ - $\pi$  and halogen bonds (Jayarajan et al., 2020; Sayin & Karakaş, 2018; Sayin & Üngördü, 2019). It is seen that compounds interact with proteins in many ways in these forms. In these pictures, polar and hydrophobic interactions are most common between compounds and cancer cell proteins.

**Table 3.** Numerical values of parameters obtained from interaction of compounds with enzymes.

	Parameter	2	3
<b>Breast cancer</b>	Docking Score	-3.57	-3.81
	Glide Ligand Efficiency	-0.14	-0.13
	Glide Hbond	-0.14	-0.16
	Glide Evdw	-26.82	-32.33
	Glide Ecoul	-0.22	-1.42
	Glide Emodel	-31.25	-39.99
<b>Liver cancer</b>	Docking Score	3.88	2.52
	Glide Ligand Efficiency	-4.93	-4.38
	Glide Hbond	-0.20	-0.15
	Glide Evdw	0.00	0.00
	Glide Ecoul	-36.26	-35.16
	Glide Emodel	2.86	2.27
<b>Lung cancer</b>	Docking Score	-43.24	-41.92
	Glide Ligand Efficiency	2.99	1.86
	Glide Hbond	-5.85	-4.28
	Glide Evdw	-0.23	-0.15
	Glide Ecoul	0.00	0.00
	Glide Emodel	-35.25	-42.62
	Glide Einternal	1.15	2.98
	Glide Emodel	-45.17	-49.21
	Glide Einternal	4.38	3.55

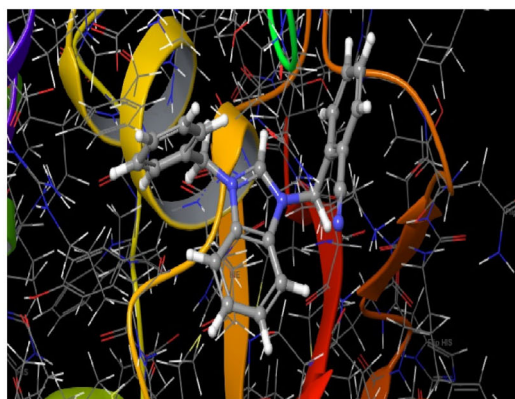
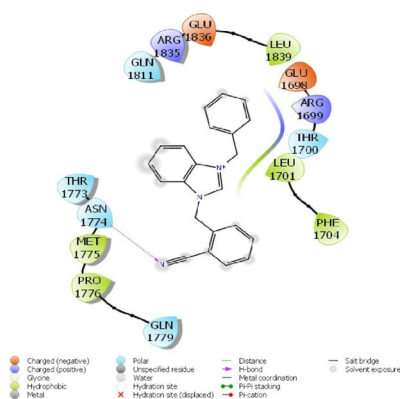


**Figure 8.** Representation of the interaction of compound 2 and breast cancer protein.

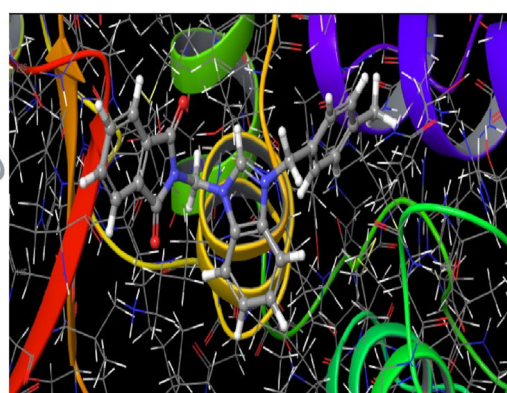
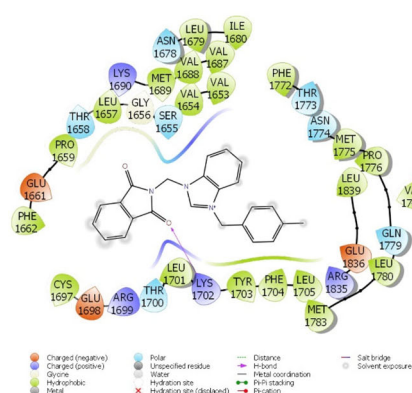


**Figure 9.** Representation of the interaction of compound 3 and breast cancer protein.

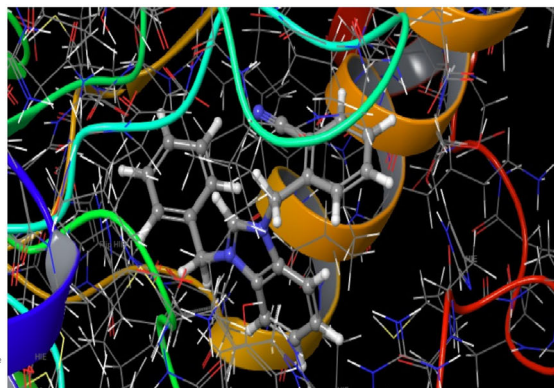
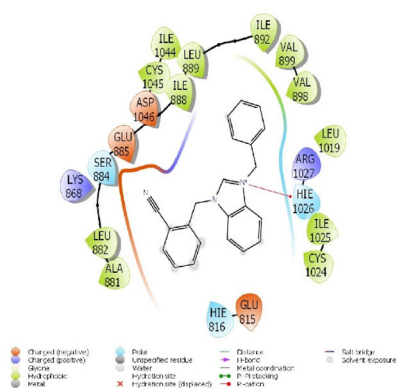


Figure 10. Representation of the interaction of compound 2 and liver cancer protein.

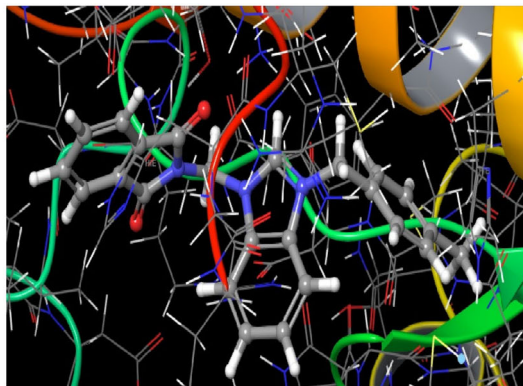
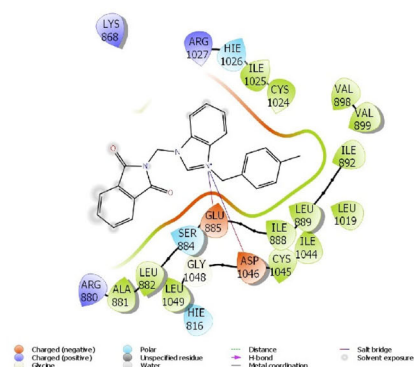


Figure 11. Representation of the interaction of compound 3 and liver cancer protein.

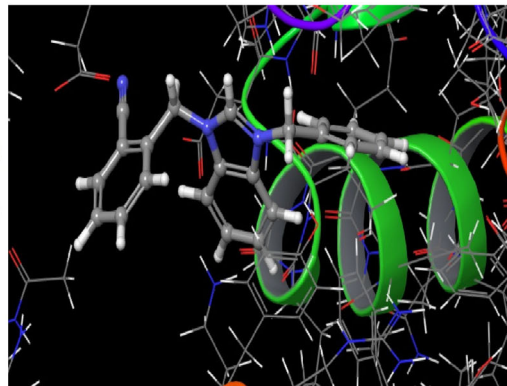
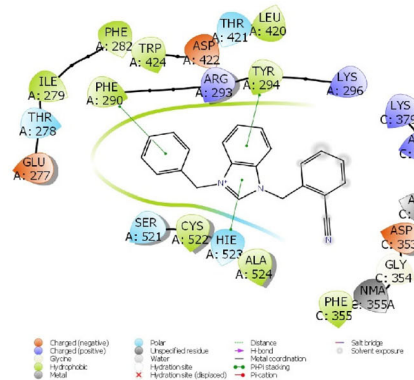


Figure 12. Representation of the interaction of compound 2 and lung cancer protein.

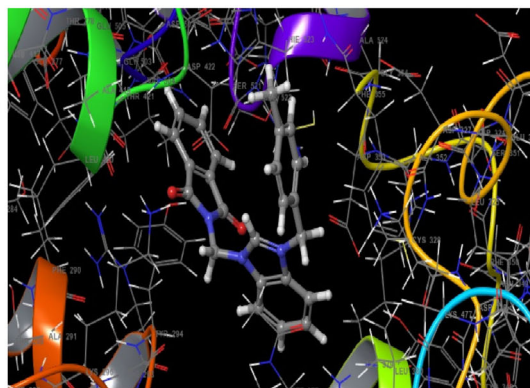
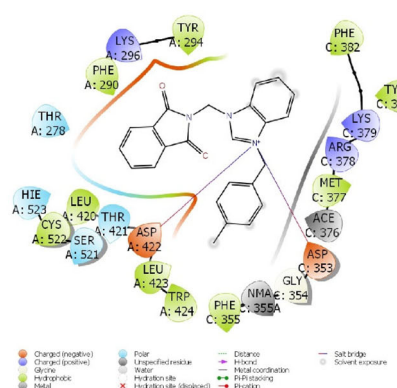


Figure 13. Representation of the interaction of compound 3 and lung cancer protein.

When the interactions of compounds with cancer proteins are examined in detail as a result of docking calculations, the N atom in the isocyanide group forms a hydrogen bond with the protein ASN 1774 against the breast cancer protein of compound **2**. Conversely, hydrophobic interactions are occurred between the  $-\text{CH}_2-\text{C}_6\text{H}_5$  group attached to the 1H-benzimidazole group together with the proteins ASN 1774 and THR 1773. In the interaction of compound **3** with breast cancer protein, there is a hydrogen bond interaction between the oxygen atom in the compound and the LYS 1702 protein. Conversely, hydrophobic interactions are occurred between the  $-\text{CH}_2-\text{C}_6\text{H}_4-\text{CH}_3$  group attached to the 1H-benzimidazole group and proteins TYR 1703, PHE 1704, LEU 1705. In the interaction of liver cancer protein with compound **2**, Pi-cation interaction is occurred between the nitrogen atom in the benzimidazole group and the HIE 1026 protein. Hydrophobic interactions are occurred between the  $-\text{CH}_2-\text{C}_6\text{H}_5$  group attached to the benzimidazole group together with the proteins ILE 1034, SN 1033 and ILE 892. In compound **3**, salt bridge interactions are occurred between the N atom in the benzimidazole group and the proteins ASP 1046 and GLU 885. Hydrophobic interactions are occurred between the  $-\text{CH}_2-\text{C}_6\text{H}_4-\text{CH}_3$  group attached to the benzimidazole group in compound **3** and proteins ILE 890, HIE 891, ILE 892, GLY 893. In the lung cancer protein, there is a Pi-Pi stacking interaction between the benzimidazole group in compound **2** and proteins TYR 294 and HIE 523. Conversely, there is a Pi-Pi stacking interaction between the  $-\text{CH}_2-\text{C}_6\text{H}_5$  group attached to the benzimidazole group and the PHE 290 protein. In compound **3**, salt bridge interactions are occurred between the nitrogen atom in the benzimidazole group and the proteins ASP 422, ASP 453. All these interactions show that comparing the biological activities of compounds against cancer proteins gives important preliminary information to the researchers before the experimental studies to be carried out. By this information, it is possible to synthesize higher and more active molecules.

#### 4. Conclusion

It is known that the resistance of pathogenic bacteria to antibiotics makes it difficult to fight infectious diseases and makes it necessary to develop new strategies to against bacteria. Nowadays, blocking communication between bacteria has become one of the promising options to combat infectious diseases. Therefore, we tested two heterocyclic organic synthesized compounds against a bacteria for learning their anti-quorum-sensing effects. The data obtained showed that compounds **2** and **3** had inhibition effects on the production of QS-regulated virulence factors, elastase, pyocyanin, biofilm formation and swarming motility in *P. aeruginosa* PA01.

Theoretical studies conducted in a pure and isolated environment are generally examined as guiding experimental studies. Experimental inputs and impurities are not found in the environment as in experimental studies. Therefore, they are very likely to give more accurate results. When they work together, they support each other. The parameters obtained from the Gaussian software and molecular docking

calculations numerically indicated that both the chemical activity and biological activity of compound **2** were higher than **3**. Consequently, this study will be a guide for future studies of these compounds.

#### Disclosure statement

No potential conflict of interest was reported by the authors.

#### Funding

The programs used in theoretical calculations were taken with the financial support of Sivas Cumhuriyet University under the project number RGD-020. In addition, TUBITAK ULAKBIM, High Performance and Grid Computing Center (TR-Grid e-Infrastructure)'s possibilities were used for theoretical calculations.

#### ORCID

Senem Akkoç  <http://orcid.org/0000-0002-1260-9425>

#### References

- Ahmed, S. A. K. S., Rudden, M., Smyth, T. J., Dooley, J. S. G., Marchant, R., & Banat, I. M. (2019). Natural quorum sensing inhibitors effectively downregulate gene expression of *Pseudomonas aeruginosa* virulence factors. *Applied Microbiology and Biotechnology*, 103(8), 3521–3535. <https://doi.org/10.1007/s00253-019-09618-0>
- Akkoç, S. (2019a). Antiproliferative activities of 2-hydroxyethyl substituted benzimidazolium salts and their palladium complexes against human cancerous cell lines. *Synthetic Communications*, 49(21), 2903–2914. <https://doi.org/10.1080/00397911.2019.1650187>
- Akkoç, S. (2019b). Derivatives of 1-(2-(piperidin-1-yl)ethyl)-1H-benzimidazole: Synthesis, characterization, determining of electronic properties and cytotoxicity studies. *ChemistrySelect*, 4(17), 4938–4943. <https://doi.org/10.1002/slct.201900353>
- Akkoç, S. (2021). Design, synthesis, characterization, and in vitro cytotoxic activity evaluation of 1,2-disubstituted benzimidazole compounds. *Journal of Physical Organic Chemistry*, 34(1), e4125.10.1002/poc.4125 <https://doi.org/10.1002/poc.4125>
- Akkoç, S., Gök, Y., Özer Lhan, I., & Kayser, V. (2016). In situ generation of efficient palladium N-heterocyclic carbene catalysts using benzimidazolium salts for the Suzuki-Miyaura cross-coupling reaction. *Current Organic Synthesis*, 13(5), 761–766. <https://doi.org/10.2174/1570179413666151218200334>
- Akkoç, S., Özer İlhan, İ., Gök, Y., Upadhyay, P. J., & Kayser, V. (2016). In vitro cytotoxic activities of new silver and PEPPSI palladium N-heterocyclic carbene complexes derived from benzimidazolium salts. *Inorganica Chimica Acta*, 449, 75–81. <https://doi.org/10.1016/j.ica.2016.05.001>
- Anantharajan, J., Zhou, H., Zhang, L., Hotz, T., Vincent, M. Y., Blevins, M. A., Jansson, A. E., Kuan, J. W. L., Ng, E. Y., Yeo, Y. K., Baburajendran, N., Lin, G., Hung, A. W., Joy, J., Patnaik, S., Marugan, J., Rudra, P., Ghosh, D., Hill, J., ... Kang, C. B. (2019). Structural and functional analyses of an allosteric EYA2 phosphatase inhibitor that has on-target effects in human lung cancer cells. *Molecular Cancer Therapeutics*, 18(9), 1484–1496. <https://doi.org/10.1158/1535-7163.MCT-18-1239>
- Asgarova, A. R., Khalilov, A. N., Brito, I., Maharramov, A. M., Shikhaliyev, N. G., Cisterna, J., Cárdenas, A., Gurbanov, A. V., Zubkov, F. I., & Mahmudov, K. T. (2019). Hydrogen and halogen bonding in the halooetherification products in chalcone. *Acta Crystallographica. Section C, Structural Chemistry*, 75(Pt 3), 342–347. <https://doi.org/10.1107/S2053229619001025>



- Becke, A. D. (1993). Density-functional thermochemistry. III. The role of exact exchange. *The Journal of Chemical Physics*, 98(7), 5648–5652. <https://doi.org/10.1063/1.464913>
- Blöcher, R., Ramírez, A. R., Castro-Escarpulli, G., Curiel-Quesada, E., & Reyes-Arellano, A. (2018). Design, synthesis, and evaluation of alkyl-quinoxalin-2(1H)-one derivatives as anti-quorum sensing molecules, inhibiting biofilm formation in *Aeromonas caviae* Sch3. *Molecules*, 23(12), 3075. <https://doi.org/10.3390/molecules23123075>
- Bratu, S., Gupta, J., & Quale, J. (2006). Expression of the las and rhl quorum-sensing systems in clinical isolates of *Pseudomonas aeruginosa* does not correlate with efflux pump expression or antimicrobial resistance. *The Journal of Antimicrobial Chemotherapy*, 58(6), 1250–1253. <https://doi.org/10.1093/jac/dkl407>
- Casilag, F., Lorenz, A., Krueger, J., Klawonn, F., Weiss, S., & Häussler, S. (2016). The LasB elastase of *Pseudomonas aeruginosa* acts in concert with alkaline protease AprA to prevent flagellin-mediated immune recognition. *Infection and Immunity*, 84(1), 162–171. <https://doi.org/10.1128/IAI.00939-15>
- Dennington, R., Keith, T., & Millam, J. (2016). *GaussView, Version 6*. Semichem Inc.
- Desai, N. C., Shihory, N. R., Kotadiya, G. M., & Desai, P. (2014). Synthesis, antibacterial and antitubercular activities of benzimidazole bearing substituted 2-pyridone motifs. *European Journal of Medicinal Chemistry*, 82, 480–489. <https://doi.org/10.1016/j.ejmech.2014.06.004>
- Du, Q., Qian, Y., Yao, X., & Xue, W. (2020). Elucidating the tight-binding mechanism of two oral anticoagulants to factor Xa by using induced-fit docking and molecular dynamics simulation. *Journal of Biomolecular Structure & Dynamics*, 38(2), 625–633. <https://doi.org/10.1080/07391102.2019.1583605>
- Essar, D. W., Eberly, L., Hadero, A., & Crawford, I. P. (1990). Identification and characterization of genes for a second anthranilate synthase in *Pseudomonas aeruginosa*: Interchangeability of the two anthranilate synthases and evolutionary implications. *Journal of Bacteriology*, 172(2), 884–900. <https://doi.org/10.1128/jb.172.2.884-900.1990>
- Fang, Y., Zhou, H., Gu, Q., & Xu, J. (2019). Synthesis and evaluation of tetrahydroisoquinoline-benzimidazole hybrids as multifunctional agents for the treatment of Alzheimer's disease. *European Journal of Medicinal Chemistry*, 167, 133–145. <https://doi.org/10.1016/j.ejmech.2019.02.008>
- Friesner, R. A., Murphy, R. B., Repasky, M. P., Frye, L. L., Greenwood, J. R., Halgren, T. A., Sanschagrin, P. C., & Mainz, D. T. (2006). Extra precision glide: Docking and scoring incorporating a model of hydrophobic enclosure for protein-ligand complexes. *Journal of Medicinal Chemistry*, 49(21), 6177–6196. <https://doi.org/10.1021/jm051256o>
- Frisch, M. J., Trucks, G. W., Schlegel, H., Scuseria, G. E., Robb, M. A., Cheeseman, J. R., Scalmani, G.; Barone, V.; Petersson, G. A.; Nakatsuji, H.; Li, X.; Caricato, M.; Marenich, A. V.; Bloino, J.; Janesko, B. G.; Gomperts, R.; Mennucci, B.; Hratchian, H. P.; Ortiz, J. V.; ... Fox, D. J. (2009). *Gaussian 09, revision D.01*. Gaussian, Inc.
- Genc Bilgiçli, H., Ergon, D., Taslimi, P., Tüzün, B., Akyazı Kuru, İ., Zengin, M., & Gülçin, İ. (2020). Novel propanolamine derivatives attached to 2-metoxifenol moiety: Synthesis, characterization, biological properties, and molecular docking studies. *Bioorganic Chemistry*, 101, 103969. <https://doi.org/10.1016/j.bioorg.2020.103969>
- Gök, Y., Akkoç, S., Çelikal, Ö. Ö., Özdemir, İ., & Günel, S. (2019). In vitro antimicrobial studies of naphthalen-1-ylmethyl substituted silver N-heterocyclic carbene complexes. *Arabian Journal of Chemistry*, 12(8), 2513–2518. <https://doi.org/10.1016/j.arabjc.2015.04.019>
- Günsel, A., Bilgiçli, A. T., Tüzün, B., Pişkin, H., Atmaca, G. Y., Erdoğan, A., & Yarasir, M. N. (2019). Synthesis of tetra-substituted phthalocyanines bearing 2-(ethyl(m-tolyl)amino)ethanol: Computational and photophysical studies. *Journal of Photochemistry and Photobiology A: Chemistry*, 373, 77–86. <https://doi.org/10.1016/j.jphotochem.2018.12.038>
- Günsel, A., Bilgiçli, A. T., Tüzün, B., Pişkin, H., Yarasir, M. N., & Gündüz, B. (2020). Optoelectronic parameters of peripherally tetra-substituted copper(II) phthalocyanines and fabrication of a photoconductive diode for various conditions. *New Journal of Chemistry*, 44(2), 369–380. <https://doi.org/10.1039/C9NJ05287A>
- Günsel, A., Kobayaoğlu, A., Bilgiçli, A. T., Tüzün, B., Tosun, B., Arabaci, G., & Yarasir, M. N. (2020). Novel biologically active metallophthalocyanines as promising antioxidant-antibacterial agents: Synthesis, characterization and computational properties. *Journal of Molecular Structure*, 1200, 127127. <https://doi.org/10.1016/j.molstruc.2019.127127>
- Hentzer, M., & Givskov, M. (2003). Pharmacological inhibition of quorum sensing for the treatment of chronic bacterial infections. *Journal of Clinical Investigation*, 112(9), 1300–1307. <https://doi.org/10.1172/JCI20074>
- Hohenstein, E. G., Chill, S. T., & Sherrill, C. D. (2008). Assessment of the performance of the M05-2X and M06-2X exchange-correlation functionals for noncovalent interactions in biomolecules. *Journal of Chemical Theory and Computation*, 4(12), 1996–2000. <https://doi.org/10.1021/ct800308k>
- Hong, S. H., Hegde, M., Kim, J., Wang, X., Jayaraman, A., & Wood, T. K. (2012). Synthetic quorum-sensing circuit to control consortial biofilm formation and dispersal in a microfluidic device. *Nature Communications*, 3(1), 613. <https://doi.org/10.1038/ncomms1616>
- Jamróz, M. H. (2004). Vibrational energy distribution analysis VEDA 4.
- Jayarajan, R., Satheeshkumar, R., Kottha, T., Subbaramanian, S., Sayin, K., & Vasuki, G. (2020). Water mediated synthesis of 6-amino-5-cyano-2-oxo-N-(pyridin-2-yl)-4-(p-tolyl)-2H-[1,2'-bipyridine]-3-carboxamide and 6-amino-5-cyano-4-(4-fluorophenyl)-2-oxo-N-(pyridin-2-yl)-2H-[1,2'-bipyridine]-3-carboxamide - An experimental and computational studies with non-linear optical (NLO) and molecular docking analyses. *Spectrochimica Acta Part A: Molecular and Biomolecular Spectroscopy*, 229, 117861. <https://doi.org/10.1016/j.saa.2019.117861>
- Jiang, Q., Chen, J., Yang, C., Yin, Y., & Yao, K. (2019). Quorum sensing: A prospective therapeutic target for bacterial diseases. *BioMed Research International*, 2019, 2015978. <https://doi.org/10.1155/2019/2015978>
- Kostylev, M., Kim, D. Y., Smalley, N. E., Salukhe, I., Greenberg, E. P., & Dandekar, A. A. (2019). Evolution of the *Pseudomonas aeruginosa* quorum-sensing hierarchy. *Proceedings of the National Academy of Sciences of the United States of America*, 116(14), 7027–7032. <https://doi.org/10.1073/pnas.1819796116>
- Kuang, Z., Hao, Y., Walling, B. E., Jeffries, J. L., Ohman, D. E., & Lau, G. W. (2011). *Pseudomonas aeruginosa* elastase provides an escape from phagocytosis by degrading the pulmonary surfactant protein-A. *PLoS One*, 6(11), e27091. <https://doi.org/10.1371/journal.pone.0027091>
- Leonid, S. (2017). Chemissan Version 4.43 Package.
- Liu, T., Cao, L., Zhang, T., & Fu, H. (2020). Molecular docking studies, anti-Alzheimer's disease, antidiabetic, and anti-acute myeloid leukemia potentials of narcissoside. *Archives of Physiology and Biochemistry*, 1–11. <https://doi.org/10.1080/13813455.2020.1828483>
- Lu, L., Hu, W., Tian, Z., Yuan, D., Yi, G., Zhou, Y., Cheng, Q., Zhu, J., & Li, M. (2019). Developing natural products as potential anti-biofilm agents. *Chinese Medicine*, 14(1), 11. <https://doi.org/10.1186/s13020-019-0232-2>
- Maharramov, A. M., Duruskari, G. S., Mammadova, G. Z., Khalilov, A. N., Aslanova, J. M., Cisterna, J., Cárdenas, A., & Brito, I. (2019). Crystal structure and hirshfeld surface analysis of (E)-5-phenyl-3-((4-(trifluoromethyl)benzylidene)amino)thiazolidin-2-iminium Bromide. *Journal of the Chilean Chemical Society*, 64(2), 4441–4447. <https://doi.org/10.4067/S0717-97072019000204441>
- Menteşe, E., Yı Imaz, F., Emirik, M., Ülker, S., & Kahveci, B. (2018). Synthesis, molecular docking and biological evaluation of some benzimidazole derivatives as potent pancreatic lipase inhibitors. *Bioorganic Chemistry*, 76, 478–486. <https://doi.org/10.1016/j.bioorg.2017.12.023>
- Morohoshi, T., Shiono, T., Takidouchi, K., Kato, M., Kato, N., Kato, J., & Ikeda, T. (2007). Inhibition of quorum sensing in *Serratia marcescens* AS-1 by synthetic analogs of N-acylhomoserine lactone. *Applied and Environmental Microbiology*, 73(20), 6339–6344. <https://doi.org/10.1128/AEM.00593-07>



- Naghiyev, F. N., Cisterna, J., Khalilov, A. N., Maharramov, A. M., Askerov, R. K., Asadov, K. A., Mamedov, I. G., Salmanli, K. S., Cárdenas, A., & Brito, I. (2020). Crystal structure and Hirshfeld surface analysis of acetacetanilide based reaction products. *Molecules*, 25(9), 2235. <https://doi.org/10.3390/molecules25092235>
- Nain, Z., Sayed, S. B., Karim, M. M., Islam, M. A., & Adhikari, U. K. (2020). Energy-optimized pharmacophore coupled virtual screening in the discovery of quorum sensing inhibitors of LasR protein of *Pseudomonas aeruginosa*. *Journal of Biomolecular Structure and Dynamics*, 38(18), 5374–5388. <https://doi.org/10.1080/07391102.2019.1700168>
- Nomura, K., Obata, K., Keira, T., Miyata, R., Hirakawa, S., Takano, K-I., Kohno, T., Sawada, N., Himi, T., & Kojima, T. (2014). *Pseudomonas aeruginosa* elastase causes transient disruption of tight junctions and downregulation of PAR-2 in human nasal epithelial cells. *Respiratory Research*, 15(1), 21.10.1186/1465-9921-15-21 <https://doi.org/10.1186/1465-9921-15-21>
- Ohman, D. E., Cryz, S. J., & Iglewski, B. H. (1980). Isolation and characterization of *Pseudomonas aeruginosa* PAO mutant that produces altered elastase. *Journal of Bacteriology*, 142(3), 836–842. <https://doi.org/10.1128/JB.142.3.836-842.1980>
- Okamoto, K., Ikemori-Kawada, M., Jestel, A., von König, K., Funahashi, Y., Matsushima, T., Tsuruoka, A., Inoue, A., & Matsui, J. (2015). Distinct binding mode of multikinase inhibitor lenvatinib revealed by biochemical characterization. *ACS Medicinal Chemistry Letters*, 6(1), 89–94. <https://doi.org/10.1021/ml500394m>
- Önem, E., Dündar, Y., Ulusoy, S., Noyanalpan, N., & Bosgelmez, T. G. (2018). Anti-quorum sensing activity of 1,3-dihydro-2h-benzimidazol-2-one derivatives. *Fresenius Environmental Bulletin*, 27(12B), 9906–9912.
- O'Toole, G. A. (2011). Microtiter dish biofilm formation assay. *Journal of Visualized Experiments*, 47(47), 2437.10.3791/2437 <https://doi.org/10.3791/2437>
- PerkinElmer. (2012). *ChemBioDraw ultra version (13.0.0.3015)*. CambridgeSoft.
- Rashid, M. H., & Kornberg, A. (2000). Inorganic polyphosphate is needed for swimming, swarming, and twitching motilities of *Pseudomonas aeruginosa*. *Proceedings of the National Academy of Sciences of the United States of America*, 97(9), 4885–4890. <https://doi.org/10.1073/pnas.060030097>
- Rasmussen, T. B., & Givskov, M. (2006). Quorum sensing inhibitors: A bargain of effects. *Microbiology (Reading, England)*, 152(Pt 4), 895–904. <https://doi.org/10.1099/mic.0.28601-0>
- Sastry, G. M., Adzhigirey, M., Day, T., Annabhimoju, R., & Sherman, W. (2013). Protein and ligand preparation: Parameters, protocols, and influence on virtual screening enrichments. *Journal of Computer-Aided Molecular Design*, 27(3), 221–234. <https://doi.org/10.1007/s10822-013-9644-8>
- Sayin, K., & Karakaş, D. (2018). Quantum chemical investigation of levofloxacin-boron complexes: A computational approach. *Journal of Molecular Structure*, 1158, 57–65. <https://doi.org/10.1016/j.molstruc.2018.01.016>
- Sayin, K., & Üngördü, A. (2019). Investigations of structural, spectral and electronic properties of enrofloxacin and boron complexes via quantum chemical calculation and molecular docking. *Spectrochimica Acta Part A: Molecular and Biomolecular Spectroscopy*, 220, 117102. <https://doi.org/10.1016/j.saa.2019.05.007>
- Schrödinger Release 2019-4. (2016). *Protein Preparation Wizard*; Epik, Schrödinger, LLC, Impact, Schrödinger, LLC, 2016; Prime, Schrödinger, LLC, 2019.
- Schrödinger Release 2019-4. (2019). LigPrep. Schrödinger, LLC.
- Schrodinger, LLC. (2019). *Small-molecule drug discovery suite 2019-4*.
- Seyhan, U., Sevil, S., Inci, C., Gulgun, B.-T., Laurent, S., Yves, Q., & Kucukguzel, S. G. (2017). Quorum sensing inhibitor activities of celecoxib derivatives in *Pseudomonas aeruginosa*. *Letters in Drug Design & Discovery*, 14(5), 613–618. <https://doi.org/10.2174/1570180814666161121120719>
- Smith, R. S., Harris, S. G., Phipps, R., & Iglewski, B. (2002). The *Pseudomonas aeruginosa* quorum-sensing molecule N-(3-oxododecanoyl)homoserine lactone contributes to virulence and induces inflammation in vivo. *Journal of Bacteriology*, 184(4), 1132–1139. <https://doi.org/10.1128/jb.184.4.1132-1139.2002>
- Stephens, P. J., Devlin, F. J., Chabalowski, C. F., & Frisch, M. J. (1994). Ab initio calculation of vibrational absorption and circular dichroism spectra using density functional force fields. *The Journal of Physical Chemistry*, 98(45), 11623–11627. <https://doi.org/10.1021/j100096a001>
- Taslimi, P., Erden, Y., Mamedov, S., Zeynalova, L., Ladokhina, N., Tas, R., Burak, T., Sujayev, A., Sadeghian, N., Alwasel, S. H., & Gulcin, I. (2020). The biological activities, molecular docking studies, and anticancer effects of 1-arylsulphonylpyrazole derivatives. *Journal of Biomolecular Structure and Dynamics*, 1–20.
- Tüzün, B. (2019). Investigation of benzimidazole derivatives as corrosion inhibitor by DFT. *Cumhuriyet Science Journal*, 40(2), 396–405. <https://doi.org/10.17776/csj.412611>
- Tüzün, B. (2020). Investigation of pyrazoly derivatives Schiff base ligands and their metal complexes used as anti-cancer drug. *Spectrochimica Acta Part A: Molecular and Biomolecular Spectroscopy*, 227, 117663. <https://doi.org/10.1016/j.saa.2019.117663>
- Vautherin, D., & Brink, D. M. (1972). Hartree-Fock calculations with Skyrme's interaction. I. Spherical nuclei. *Physical Review C*, 5(3), 626–647. <https://doi.org/10.1103/PhysRevC.5.626>
- Venturi, V. (2006). Regulation of quorum sensing in *Pseudomonas*. *FEMS Microbiology Reviews*, 30(2), 274–291. <https://doi.org/10.1111/j.1574-6976.2005.00012.x>
- Wang, W., Morohoshi, T., Ikeda, T., & Chen, L. (2008). Inhibition of Lux quorum-sensing system by synthetic N-acyl-L-homoserine lactone analogues. *Acta Biochimica et Biophysica Sinica*, 40(12), 1023–1028. <https://doi.org/10.1111/j.1745-7270.2008.00490.x>
- Wiberg, K. B. (2004). Basis set effects on calculated geometries: 6-311++G\*\* vs. aug-cc-pVDZ. *Journal of Computational Chemistry*, 25(11), 1342–1346. <https://doi.org/10.1002/jcc.20058>
- Williams, R. S., Green, R., & Glover, J. N. (2001). Crystal structure of the BRCT repeat region from the breast cancer-associated protein BRCA1. *Nature Structural Biology*, 8(10), 838–842. <https://doi.org/10.1038/nsb1001-838>
- Yadigarov, R. R., Khalilov, A. N., Mamedov, I. G., Nagiev, F. N., Magerramov, A. M., & Allakhverdiev, M. A. (2009). Reaction of 3-chloro-1-(2,4,6-trimethylphenyl)propan-2-one with amines. *Russian Journal of Organic Chemistry*, 45(12), 1856–1858. <https://doi.org/10.1134/S1070428009120185>
- Yin, J., Khalilov, A. N., Muthupandi, P., Ladd, R., & Birman, V. B. (2020). Phenazine-1,6-dicarboxamides: Redox-responsive molecular switches. *Journal of the American Chemical Society*, 142(1), 60–63. <https://doi.org/10.1021/jacs.9b11160>